Magn Reson Mater Phy (2018) 31:415–424
https://doi.org/10.1007/s10334-017-0659-3

RESEARCH ARTICLE

T_2 mapping of cerebrospinal fluid: 3 T versus 7 T

Jolanda M. Spijkerman[1] · Esben T. Petersen[2] · Jeroen Hendrikse[1] · Peter Luijten[1] · Jaco J. M. Zwanenburg[1]

Received: 6 July 2017 / Revised: 22 September 2017 / Accepted: 13 October 2017 / Published online: 6 November 2017

Abstract
Object Cerebrospinal fluid (CSF) T_2 mapping can potentially be used to investigate CSF composition. A previously proposed CSF T_2–mapping method reported a T_2 difference between peripheral and ventricular CSF, and suggested that this reflected different CSF compositions. We studied the performance of this method at 7 T and evaluated the influence of partial volume and $\boldsymbol{B}_1$ and $\boldsymbol{B}_0$ inhomogeneity.
Materials and methods T_2-preparation-based CSF T_2-mapping was performed in seven healthy volunteers at 7 and 3 T, and was compared with a single echo spin-echo sequence with various echo times. The influence of partial volume was assessed by our analyzing the longest echo times only. $\boldsymbol{B}_1$ and $\boldsymbol{B}_0$ maps were acquired. $\boldsymbol{B}_1$ and $\boldsymbol{B}_0$ dependency of the sequences was tested with a phantom.
Results $T_{2,\mathrm{CSF}}$ was shorter at 7 T compared with 3 T. At 3 T, but not at 7 T, peripheral $T_{2,\mathrm{CSF}}$ was significantly shorter than ventricular $T_{2,\mathrm{CSF}}$. Partial volume contributed to this T_2 difference, but could not fully explain it. $\boldsymbol{B}_1$ and $\boldsymbol{B}_0$ inhomogeneity had only a very limited effect. $T_{2,\mathrm{CSF}}$ did not depend on the voxel size, probably because of the used method to select of the regions of interest.
Conclusion CSF T_2 mapping is feasible at 7 T. The shorter peripheral $T_{2,\mathrm{CSF}}$ is likely a combined effect of partial volume and CSF composition.

Keywords Cerebrospinal fluid · T2 relaxation · 7 T · 3 T · MRI

Introduction

Qin [1] proposed a fast 3-T MRI method to map the volume and T_2 of cerebrospinal fluid (CSF) in the brain. A striking finding with this method was the observation of a shorter T_2 in the peripheral CSF compared with the T_2 of the CSF in the lateral ventricles. Qin suggested that this T_2 difference is caused by differences in CSF composition between both areas, implying that CSF T_2 ($T_{2,\mathrm{CSF}}$) can be used as a noninvasive biomarker for CSF composition. This would be highly relevant in the light of the recent attention to the clearance of brain waste products, in which CSF is involved [2–5]. A method that can noninvasively assess CSF composition would provide a noninvasive window on the brain clearance system, with great potential for applications in studying diseases related to dementia such as Alzheimer's disease and cerebral small vessel disease. If $T_{2,\mathrm{CSF}}$ is indeed useful as a functional marker of the brain clearance system, it could be studied next to other advanced imaging markers of early brain damage such as microbleeds, microinfarcts, and hippocampus subfield volumes and atrophy. As many of these advanced markers are acquired at 7 T [6–8], it is desirable to implement and evaluate CSF T_2 mapping at 7 T as well.

At 7 T, $\boldsymbol{B}_1$ inhomogeneity is considerable and may influence the T_2 mapping results, despite the relative $\boldsymbol{B}_1$ insensitivity of the used CSF T_2 mapping method. Even at 3 T, considerable $\boldsymbol{B}_1$ inhomogeneity in the brain can

Electronic supplementary material The online version of this article (doi:10.1007/s10334-017-0659-3) contains supplementary material, which is available to authorized users.

✉ Jolanda M. Spijkerman
j.m.spijkerman-2@umcutrecht.nl

1 Department of Radiology, University Medical Center Utrecht, HP E 01.132, P.O.Box 85500, 3508 GA Utrecht, The Netherlands

2 Danish Research Centre for Magnetic Resonance, Centre for Functional and Diagnostic Imaging and Research, Copenhagen University Hospital Hvidovre, 2650 Hvidovre, Denmark

be observed [9]. Also, when T_2 is measured in peripheral CSF, partial volume effects with tissue cannot be avoided. So, we hypothesized that these partial volume effects and $\boldsymbol{B}_1$ imperfections can explain the previously observed T_2 differences. De Vis et al. [10] obtained a rough estimation of the influence of partial volume effects on the estimated $T_{2,\mathrm{CSF}}$ by scanning with two different resolutions. The higher resolution resulted in longer T_2 times, suggesting a role for partial volume effects. Because the influence of $\boldsymbol{B}_1$ inhomogeneity and partial volume effects is not clear yet, it remains uncertain to what extent $T_{2,\mathrm{CSF}}$ can be used to assess the composition of CSF.

In this work we studied the performance of Qin's CSF T_2 mapping method at 7 T. The specific goals were to investigate the influence of $\boldsymbol{B}_1$ and $\boldsymbol{B}_0$ imperfections on the estimated $T_{2,\mathrm{CSF}}$, to assess the influence of partial volume effects, and to evaluate to what extent the previously observed difference in $T_{2,\mathrm{CSF}}$ between periphery and ventricles can be explained by $\boldsymbol{B}_1$, $\boldsymbol{B}_0$, and partial volume effects. $\boldsymbol{B}_1$ and $\boldsymbol{B}_0$ sensitivity was investigated with phantom measurements, and by comparison of the method for 7 and 3 T in healthy humans. Partial volume effects were estimated by removal of the influence of partial volume with tissue, through selection of only the last (longest) echo times (TEs). Also, scanning was done at different resolutions.

Materials and methods

Sequence

The CSF T_2 mapping sequence used in this research is based on T_2 preparation, and has been described elsewhere [1, 10]. For this study the method was further extended to improve the fit reliability of the long T_2 times by implementation of longer refocusing pulse trains, yielding longer TEs. Briefly, the sequence consists of four parts (Fig. 1). First, a set of four nonselective water suppression enhanced through T_1 effects (WET) pulses are applied for saturation to prevent slice history effects. These pulses are optimized for saturation of free water (applicable for T_1 between 3 and 6 s); the pulse angles are 156°, 71°, 109°, and 90° [11]. Second, a delay time (T_{delay}) follows, where T_1 relaxation occurs, followed by crusher gradients. Third, T_2 preparation is applied, consisting of a nonselective 90° pulse, a set of 4, 8, 16, or 32 nonselective refocusing pulses (R) according to the Malcolm Levitt (MLEV) phase cycling scheme, and a nonselective −90° pulse with a crusher gradient to crush any remaining transverse magnetization [12]. Each refocusing pulse R is a composite pulse, consisting of 90°_x, 180°_y, 90°_x rectangular pulses (or the inverse $\bar{R}$: 90°_{-x}, 180°_{-y}, 90°_{-x}). The duration of a single refocusing pulse was 2.6 ms. T_2 relaxation occurs

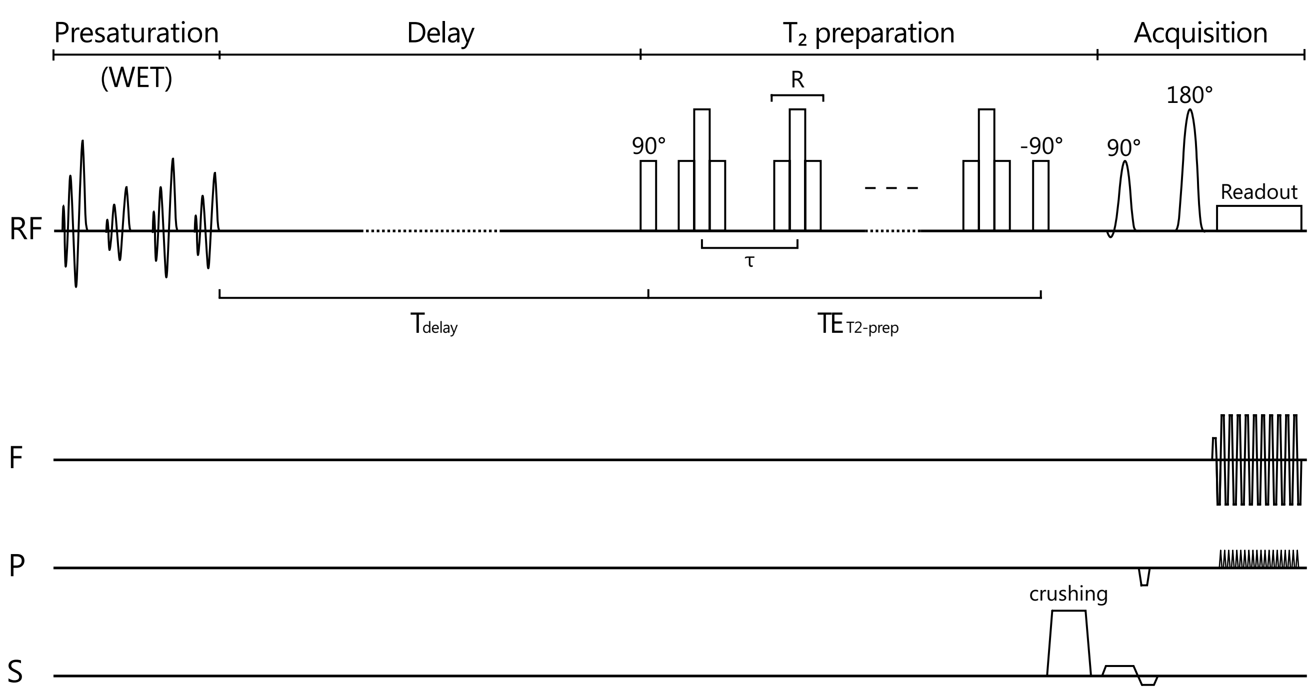

Fig. 1 Cerebrospinal fluid T_2 mapping pulse sequence. The sequence consists of four parts: water suppression enhanced through T_1 effects (WET) presaturation, a fixed delay with duration T_{delay}, a T_2 preparation module with Malcolm Levitt (MLEV) phase cycling, and a spin echo echo planar imaging (SE-EPI) image acquisition. T_2 relaxation occurs during $\mathrm{TE}_{\mathrm{T2\text{-}prep}}$. To perform T_2 mapping the sequence was repeated, while the number of refocusing pulses (and therefore $\mathrm{TE}_{\mathrm{T2\text{-}prep}}$) was increased for a fixed interpulse delay τ. The applied RF pulses are shown on the RF axis, and the applied gradients are shown on the frequency (F), phase (P), and slice (S) encoding axes

during $TE_{T2\text{-prep}}$, which is determined by the number of refocusing pulses and the spacing between the centers of the refocusing pulses (τ). To achieve long $TE_{T2\text{-prep}}$ times, τ was chosen as 150 ms. This resulted in $TE_{T2\text{-prep}}$ durations of 600, 1200, 2400, and 4800 ms. Also, one scan was acquired without any refocusing pulses; this scan was not used in data analysis. The fourth part of the sequence is a single-shot 2D spin echo (SE) echo planar imaging (EPI) readout. During the EPI train, T_2 decay also occurs; this can, however, be regarded as a constant factor, and was therefore disregarded in the analysis.

Although the refocusing train in the T_2 preparation is relatively insensitive to $\boldsymbol{B}_1$ inhomogeneities because of the MLEV phase cycling scheme, the 90° rectangular pulses before and after the train may fail in the case of $\boldsymbol{B}_1$ deviations. Consequently, we hypothesized that a fraction of the magnetization may be unaffected by the T_2-preparation module, which could have a relatively large impact on the measured signal in the case of partial volume effects. Also, in the case of imperfect $\boldsymbol{B}_1$, T_1-weighted stimulated echoes may influence the T_2 measurements, although this effect is expected to be relatively small because of the long T_1 of CSF (4.4 s [13]). Therefore, T_2 mapping with a single echo SE-EPI sequence with various TEs was used as a truly $\boldsymbol{B}_1$-insensitive reference (shown in the electronic supplemental material).

Nonselective pulses were used where possible to minimize motion sensitivity. Consequently, only the excitation pulse of the SE-EPI readout was selective.

Phantom measurements

Phantom measurements were performed to test the $\boldsymbol{B}_1$ and $\boldsymbol{B}_0$ sensitivity. The experiments were performed with a 7-T Philips Achieva scanner (Philips Medical Systems, Best, Netherlands) with a 32-channel head coil (Nova Medical, Wilmington, MA, USA), with a tap water phantom at room temperature. The phantom size was 200 × 95 × 20 mm^3. The phantom was scanned with the same TEs as used for the in vivo experiments. A single slice was acquired with 3 × 3 × 6 mm^3 resolution, field of view (FOV) of 240 × 96 mm^2, T_{delay} of 15 s, [which is more than three times the T_1 of CSF (4.4 s [13])], and sensitivity encoding (SENSE) [14] (with SENSE factor 1, meaning that the coil sensitivities of the receive coils were used for optimal coil combination without imaging acceleration). A series of T_2 maps with increasing through-plane $\boldsymbol{B}_0$ gradients were acquired to study the effect of diffusion for $\boldsymbol{B}_1$ of 100%. The following through-plane $\boldsymbol{B}_0$ gradient strengths were applied by addition of this strength to the linear shim term in the user interface: 0, 0.05, 0.1, 0.2, 0.3, and 0.5 mT/m. The phantom appeared sensitive to free induction decay (FID) artifacts, because of the relatively large volume of water and more pronounced $\boldsymbol{B}_1$ inhomogeneity [15]. The acquisition with the highest $\boldsymbol{B}_0$ gradient yielded images free of FID artifacts, which allowed us to study the $\boldsymbol{B}_1$ dependency of the CSF T_2 mapping sequence. $\boldsymbol{B}_0$ and $\boldsymbol{B}_1$ maps were acquired, with use of identical resolution and FOV as for the T_2 mapping acquisitions. The $\boldsymbol{B}_0$ map was obtained with a gradient echo sequence with two different TEs (1.64 and 2.64 ms). The $\boldsymbol{B}_1$ mapping sequence was based on the actual flip angle method [16], with first repetition time (TR) of 40 ms, second TR of 160 ms, TE of 0.96 ms, and a flip angle of 50°.

In vivo measurements

In vivo experiments were performed at both 7 and 3 T to test the feasibility of CSF T_2 mapping at 7 T, to further assess the sensitivity to $\boldsymbol{B}_1$ inhomogeneities, and to explore the influence of partial volume effects. Seven healthy volunteers (three men, mean age 34 ± 11 years, age range 21–54 years) participated in this study. Informed consent was given by all volunteers in accordance with the requirements of the Institutional Review Board of the University Medical Center Utrecht (Utrecht, Netherlands). All volunteers were scanned with both a 3-T Philips Achieva scanner with an eight-channel head coil (Philips Healthcare, Best, Netherlands) and the 7-T scanner that was also used for the phantom study. The CSF T_2 mapping scans were acquired in a single coronal slice, planned through both the lateral ventricles and the fourth ventricle (Fig. 2a). The scanning parameters are summarized in Table 1. The fixed T_{delay} was 15 s, and TR ranged between 20 and 25 s depending on $TE_{T2\text{-prep}}$. Other parameters were as follows: SENSE factor 2.3 in the left–right direction and FOV of 240 × 240 mm^2. Because of the long TR, the specific absorption rate (SAR) remained well within the specific absorption rate limits, also at 7 T. No additional methods were used to correct the scans for eddy currents. The low bandwidth of the scan may cause distortions in areas with poor shimming, such as the nasal cavities. However, shimming was good in the selected coronal slice. Also $\boldsymbol{B}_0$ and $\boldsymbol{B}_1$ maps were acquired.

Data analysis

Phantom

The resulting T_2 estimates were analyzed as a function of $\boldsymbol{B}_1$ and $\boldsymbol{B}_0$. $\boldsymbol{B}_1$ sensitivity was assessed with use of the scans with the highest $\boldsymbol{B}_0$ gradient strength (0.5 mT/m), where no FID artifacts were present. The $\boldsymbol{B}_1$ range present in the scan was used. On the basis of $\boldsymbol{B}_1$ in each voxel, the voxels were sorted over eight bins of 5% $\boldsymbol{B}_1$, leading to $\boldsymbol{B}_1$ bins ranging from (85 ± 2.5)% to (120 ± 2.5)%. The signal was averaged over each $\boldsymbol{B}_1$ bin, and T_2 values were fitted over this averaged signal. $\boldsymbol{B}_0$ sensitivity was assessed with the

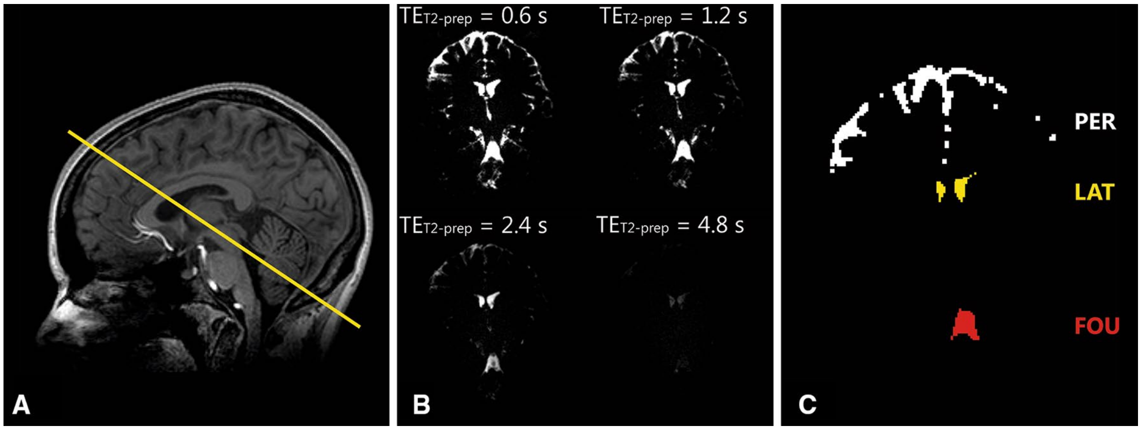

Fig. 2 **a** Planning of the cerebrospinal fluid (CSF) T_2 mapping scans, through the lateral ventricles and the fourth ventricle. **b** CSF T_2 mapping scans at 7 T for increasing echo times ($TE_{T2\text{-prep}}$) (0.6, 1.2, 2.4, and 4.8 s), shown with equal intensity scaling. **c** The region of interest masks used: the periphery (PER; white), the lateral ventricles (LAT; yellow), and the fourth ventricle (FOU; red)

Table 1 Scan parameters used for the in vivo experiments for the cerebrospinal fluid T_2 mapping sequence (based on T_2 preparation)

	Resolution (mm^3)	$TE_{readout}$ (ms)	$TE_{T2\text{-prep}}$ (ms)	EPI factor	Bandwidth (phase/frequency) (Hz/voxel)	Scan duration (min)
3 T	1 × 1 × 4	133	0–4800[a]	105	8.1/961	2:59
	3 × 3 × 6	42	0–4800[a]	67	28.2/2308	2:59
7 T	1 × 1 × 2	127	0–4800[a]	107	8.4/1082	3:04
	1 × 1 × 4	126	0–4800[a]	107	8.4/1082	3:04
	3 × 3 × 6	23	0–4800[a]	37	55.1/2642	3:04

EPI echo planar imaging, *TE* echo time, $TE_{T2\text{-prep}}$ echo time of T_2-preparation

[a] The $TE_{T2\text{-prep}}$ values used were 0, 600, 1200, 2400, and 4800 ms.

various applied $\boldsymbol{B}_0$ gradient strengths (0, 0.05, 0.1, 0.2, 0.3, and 0.5 mT/m). In each scan, only voxels with $\boldsymbol{B}_1$ between 97.5% and 102.5% were included. An additional intensity threshold was applied on the scan with the longest $TE_{T2\text{-prep}}$ to minimize the influence of artifacts in the lower $\boldsymbol{B}_0$ gradient scans. This threshold was set at 75% of the maximum intensity for the longest TE. The signal of all voxels included was averaged over each scan, and T_2 values were fitted over this averaged signal.

In vivo

Three regions of interest (ROIs) were defined on the acquired in vivo scans: the lateral ventricles, the fourth ventricle, and peripheral CSF. The ROI masks were made by our applying an intensity threshold to the first TE ($TE_{T2\text{-prep}} = 0.6$ s). The intensity threshold was set at 25% of the maximum intensity in the image. Figure 2b and c shows the acquired CSF T_2 mapping scan at 7 T with a resolution of $1 \times 1 \times 4$ mm^3 at all TEs for one volunteer, and the ROIs used. Conservative ROIs were used in the ventricles by our eroding the intensity-based ROIs with one voxel to minimize both partial volume and motion sensitivity. Erosion of the peripheral ROIs was not feasible.

The signal was averaged over each ROI, and T_2 values were fitted over this averaged signal, with use of a single exponential decay model. Also mean $\boldsymbol{B}_0$ and $\boldsymbol{B}_1$ values were determined for each ROI. To minimize the influence of, for example, motion or partial volume effects on the data analysis, only fit results with R^2 of 0.99 or higher were considered.

Partial volume assessment

In the peripheral CSF an additional assessment of the influence of partial volume was made by our performing a partial volume correction. Only $TE_{T2\text{-prep}}$ values of at least 1200 ms (excluding the shortest $TE_{T2\text{-prep}}$ of 600 ms) were taken into account in the analysis. Thereby, maximal nulling of, for example, tissue signal was achieved, since the T_2 values of tissue are below 100 ms [17, 18], about ten times shorter than the minimal $TE_{T2\text{-prep}}$ used. The analysis with only the last $TE_{T2\text{-prep}}$ times was also performed on the phantom scans to check for any systematic errors for all $\boldsymbol{B}_0$ gradient strengths applied and $\boldsymbol{B}_1$ between 97.5% and 102.5%.

All data analysis was performed in MATLAB (version 2015B, The MathWorks, Natick, MA, USA). IBM SPSS Statistics (version 21.0) was used for statistical analysis. Median $T_{2,\mathrm{CSF}}$ values and full ranges are reported. Wilcoxon signed-rank tests (significance level $p < 0.05$) were used to compare CSF T_2 values in the lateral and fourth ventricles with those in the periphery to explore the observed T_2 differences.

Results

Phantom measurements

Figure 3 shows the results of the phantom measurements for the $\boldsymbol{B}_1$ dependency (Fig. 3a) and $\boldsymbol{B}_0$ gradient dependency (Fig. 3b). The CSF T_2 mapping sequence measured a T_2 of 1.71 s (95% confidence interval 1.66–1.76 s) for $\boldsymbol{B}_1$ of (100 ± 2.5)% and $\boldsymbol{B}_0$ gradient strength of 0 mT/m. The sequence showed only minor $\boldsymbol{B}_1$ sensitivity (assessed in the scans with $\boldsymbol{B}_0$ gradient strength of 0.5 mT/m), with T_2 ranging from 1.41 s (95% confidence interval 1.38–1.43 s) at $\boldsymbol{B}_1$ of (85 ± 2.5)% to 1.49 s (95% confidence interval 1.40–1.57 s) at $\boldsymbol{B}_1$ of (105 ± 2.5)%. Also minor $\boldsymbol{B}_0$ gradient dependency was observed.

In vivo measurements

Thirty-five CSF T_2 mapping scans were acquired, for both field strengths and the different resolutions. Per scan, three fits were made, one per ROI, resulting in a total of 105 fits (42 at 3 T, 63 at 7 T). On the basis of the strict requirement on minimum R^2, 14 fits were excluded (four at 3 T, ten at 7 T), which corresponds to 13% of the total number of fits (10% at 3 T, 16% at 7 T); see Table 2 for a detailed overview.

The in vivo results for the scans with a resolution of $1 \times 1 \times 4$ mm^3 are summarized in Fig. 4. The results for the other resolutions were not significantly different from the data shown here (all data are shown in Tables S3, S4, S5). Although T_2 differences between the resolutions were not significant, in most cases the shortest T_2 times were observed for the largest voxel sizes.

At 7 T significantly shorter T_2 times were found compared with at 3 T. At 3 T the T_2 times measured in the periphery were significantly shorter than those measured in the lateral and fourth ventricles. The T_2 times measured at 7 T were not significantly different between the three ROIs. At 3 T the median $\boldsymbol{B}_1$ in the periphery was 85% (range 79–90%), while in the lateral and fourth ventricles it was 109% (ranges

Table 2 Number of scans acquired and T_2 fits performed, and the number of excluded T_2 fits per region of interest

Resolution (mm^3)	Scans	Fits	Excluded fits		
			Lateral ventricles	Fourth ventricle	Periphery
3 T					
$1 \times 1 \times 4$	7	21	0	1	0
$3 \times 3 \times 6$	7	21	2	1	0
Total	14	42	2	2	0
7 T					
$1 \times 1 \times 2$	7	21	0	1	0
$1 \times 1 \times 4$	7	21	1	3	0
$3 \times 3 \times 6$	7	21	1	4	0
Total	21	63	2	8	0

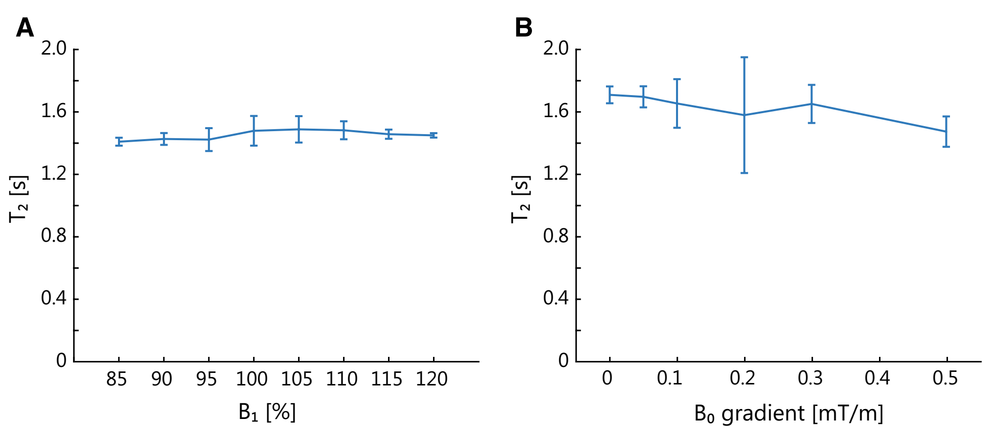

Fig. 3 Results of the phantom measurements for the B_1 (**a**) and $\boldsymbol{B}_0$ gradient dependency (**b**) showing the fitted T_2 for different $\boldsymbol{B}_1$ values and through-plane $\boldsymbol{B}_0$ gradient strengths, respectively. The error bars show the 95% confidence interval of the fitted T_2. The cerebrospinal fluid T_2 mapping sequence shows only minor sensitivity to $\boldsymbol{B}_1$ and to the through-plane $\boldsymbol{B}_0$ gradient (and thus to diffusion). The effect of the $\boldsymbol{B}_0$ gradient was most apparent for the highest $\boldsymbol{B}_0$ gradient. The $\boldsymbol{B}_1$ dependency was determined with a $\boldsymbol{B}_0$ gradient strength of 0.5 mT/m to avoid free induction decay (FID) artifacts in regions with $\boldsymbol{B}_1$ deviating from 100%. For a $\boldsymbol{B}_0$ gradient of 0.2 mT/m, the confidence interval was greater because of FID artifacts

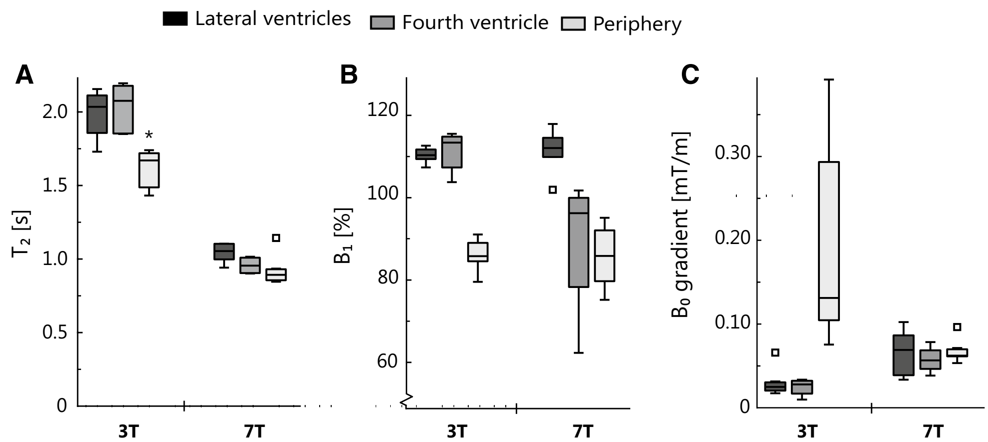

Fig. 4 In vivo results: T_2 (**a**), $\boldsymbol{B}_1$ (**b**), and $\boldsymbol{B}_0$ gradient (**c**) for the three different regions of interest. Outliers are represented by a square. Significant differences in measured T_2 were found between the periphery and the lateral and fourth ventricles at 3 T (indicated by an asterisk)

106–112% and 103–114%). The median $\boldsymbol{B}_0$ gradient in the periphery was 0.13 mT/m (range 0.07–0.38 mT/m), while in the lateral and fourth ventricles it was 0.02 and 0.03 mT/m, respectively (range 0.02–0.06 mT/m and 0.01–0.03 mT/m, respectively). At 7 T, lower $\boldsymbol{B}_1$ values were observed in the periphery and the fourth ventricle [median 86% (range 75–94%) and 93% (range 62–101%), respectively], and higher $\boldsymbol{B}_1$ values were observed in the lateral ventricles [median 111% (range 109–116)]. Similar $\boldsymbol{B}_0$ gradients were observed in the three ROIs [median 0.07 mT/m (range 0.03–0.10 mT/m), 0.06 mT/m (range 0.04–0.08 mT/m), and 0.06 mT/m (range 0.05–0.09 mT/m), for the lateral ventricles, the fourth ventricle, and the periphery, respectively].

Partial volume assessment

Figure 5 shows the results for the additional analysis of peripheral CSF to assess the influence of partial volume. The partial volume correction resulted in longer T_2 times, with a significant increase of 118 ms at both 3 and 7 T. At 7 T the corrected peripheral CSF T_2 was quite similar to the ventricular T_2 (1.01 s vs 1.05 s), while at 3 T the mean peripheral T_2 was still approximately 200 ms shorter than the ventricular T_2 times [1.79 s (range 1.49–1.82 s) vs 2.03 s (range 1.73–2.16 s), $p = 0.02$]. The results for this analysis of the phantom data are shown in Fig. 6. Both analysis methods (including all TEs or only the longest TEs) resulted in similar T_2 values, indicating no systematic errors in the additional analysis with only the longest TEs.

Discussion

In this research we have shown the feasibility of CSF T_2 mapping at 7 T with a dedicated CSF T_2 mapping sequence based on T_2 preparation, which was initially developed at

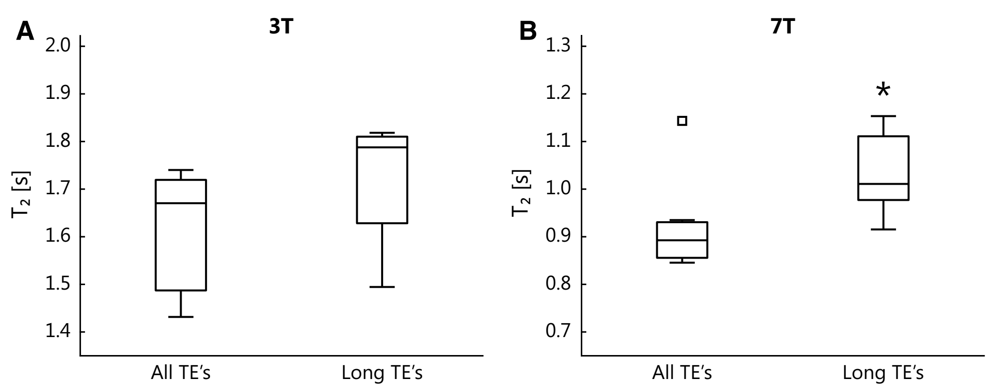

Fig. 5 T_2 values of peripheral cerebrospinal fluid resulting from the use of only the longest echo times (TEs) compared with the original analysis. Outliers are represented by a square. At both 3 and 7 T an increase in T_2 can be observed. The asterisk indicates a significant difference with the original analysis (including all TEs)

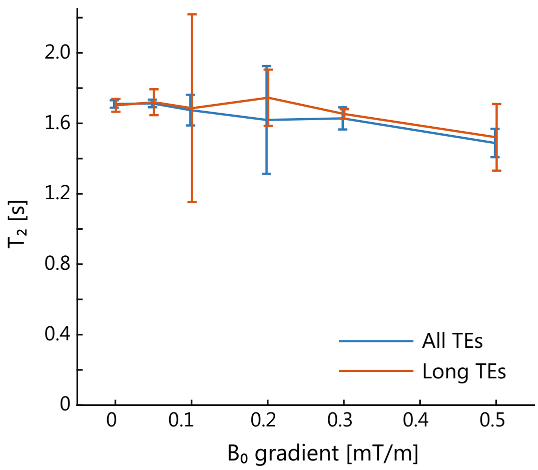

Fig. 6 T_2 values of the phantom, resulting from the use of only the longest echo times (TEs; orange) compared with the original analysis (blue). Both analyses result in similar T_2 values

3 T. We investigated the sensitivity of this sequence for the influence of $\boldsymbol{B}_1$, diffusion ($\boldsymbol{B}_0$ gradient), and partial volume effects. The sequence appeared to be relatively insensitive to $\boldsymbol{B}_1$ and $\boldsymbol{B}_0$ inhomogeneity. Partial volume effects tend to lower the observed T_2 values at the periphery. $T_{2,\mathrm{CSF}}$ was considerably shorter at 7 T than at 3 T in all three ROIs. The peripheral $T_{2,\mathrm{CSF}}$ was significantly shorter than the ventricular $T_{2,\mathrm{CSF}}$ at 3 T (but not at 7 T).

The peripheral $T_{2,\mathrm{CSF}}$ increased considerably on partial volume correction, as obtained from analysis of long TEs (more than ten times the tissue T_2). The partial volume correction for the SE-EPI sequence, which was used as a relatively $\boldsymbol{B}_1$-insensitive reference (data shown in the electronic supplementary material), did not significantly increase T_2 values, although the SE-EPI sequence showed an even larger T_2 difference between the periphery and ventricles. The ventricular T_2 values measured with the CSF T_2 mapping sequence at 3 T match with T_2 values found in literature [1, 10, 19, 20]. Given the results from our measurements and analysis, we believe that the observed T_2 difference between the ventricular and peripheral CSF could be partly due to physiological differences. However, the different results for different sequences and field strengths and the confounding influence of partial volume effects will make it challenging to accurately isolate and quantify any true physiological effect from confounders. This will hamper applications in research focusing on in vivo evaluation of the (regional) composition of CSF.

B_1 and B_0 dependency

In the phantom measurements only minor $\boldsymbol{B}_1$ dependency was found for the CSF T_2 mapping sequence, as shown in Fig. 3a. Also, the measurements with an increasing through-plane $\boldsymbol{B}_0$ gradient showed only limited $\boldsymbol{B}_0$ gradient dependency, except for the highest $\boldsymbol{B}_0$ gradient (0.5 mT/m), as shown in Fig. 3b. In the in vivo measurements, the $\boldsymbol{B}_0$ gradient was similar between the periphery and the ventricles at 7 T, and differed by a maximum of 0.38 mT/m (median $\boldsymbol{B}_0$ gradient was 0.13 mT/m) at 3 T (Fig. 4c). This difference in $\boldsymbol{B}_0$ homogeneity between 3 and 7 T is probably due to different shimming techniques: image-based third-order shimming was used at 7 T, and linear shimming was used at 3 T. The low sensitivity to $\boldsymbol{B}_0$ gradient shows that the T_2 mapping sequence is relatively insensitive to diffusion. It is not likely that $\boldsymbol{B}_0$ gradients due to imperfect shimming contributed considerably to the observed difference in T_2 between periphery and ventricles.

Partial volume effects

The different resolutions used at both field strengths did not yield considerably different T_2 values (Tables S3, S4, S5), although there is a trend of longer measured ventricular T_2 times for smaller voxel sizes at 3 T, similarly to what was found by to De Vis et al. [10]. As the ventricular ROIs were eroded, the voxels at the edges, where more partial volume is expected, were discarded. For the periphery, however, erosion was not feasible because of the thin shape of the ROI. Moreover, the ROI definition was based on an intensity threshold, which depends on the CSF fraction in each voxel. Since the total subarachnoidal CSF volume is quite small, and distributed over a relatively large area [21], partial volume is probably present in all peripheral ROIs, independently of the voxel sizes used in this work.

The role of partial volume effects regarding the measured peripheral $T_{2,\mathrm{CSF}}$ was investigated by use of the longest TEs only (Fig. 5) to maximally remove the influence of partial volume. It could seem unexpected that the use of the late TEs reveals a considerable partial volume effect, since the first $\mathrm{TE}_{\mathrm{T2\text{-}prep}}$ is already relatively long compared with the tissue T_2. The T_2 of gray matter is approximately 90 ms at 3 T [18, 22] and 55 ms at 7 T [18, 23], while the first TE was 600 ms. However, it is possible that partial volume occurs with a compartment with a relatively long T_2 in the cerebral cortex, like arterial blood (T_2 around 150 ms at 3 T [24, 25]) or the outer rim of the cortex (unknown but long T_2, greater than 100 ms, at 7 T [26]). At the shortest $\mathrm{TE}_{\mathrm{T2prep}}$ (600 ms), the signal of arterial blood has decayed to 2%. However, in the case of small partial volume fractions of CSF in the periphery, this could still have a considerable influence on the measured T_2. The outer layer of the cerebral cortex (layer I) may have a long T_2 because it contains almost no neuronal cell bodies, and many glial cells instead, similarly to gliotic lesions, which also have a long T_2 [26].

Peripheral versus ventricular CSF T_2 and field strength dependence

De Vis et al. [10] found a T_2 difference of 609 ± 133 ms between the periphery and the ventricles at 3 T, and Qin found a T_2 difference of 420 ± 155 ms at 3 T. Also in this work a shorter $T_{2,\mathrm{CSF}}$ was measured in the periphery compared with the ventricles, as shown in Fig. 4a. This T_2 difference is larger at 3 T than at 7 T: the T_2 difference is 365 ms at 3 T and 161 ms at 7 T, which corresponds to differences of 18% and 15% relative to the T_2 in the lateral ventricles for 3 and 7 T, respectively. Partial volume correction, which led to a peripheral CSF T_2 increase of 118 ms at both field strengths (Fig. 5), resulted in remaining T_2 differences of 247 ms and only 43 ms for 3 and 7 T, respectively. These correspond to a T_2 difference of 12% and 4% relative to the ventricular CSF T_2 for 3 and 7 T, respectively. A relatively larger T_2 difference was found when a SE-EPI sequence was used, and remained largely unchanged after partial volume correction (data shown in the electronic supplementary material).

These results indicate a true T_2 difference between peripheral and ventricular CSF. A potential physiological explanation for this observed T_2 difference could be sought in differences in, for example, in the levels of O_2, protein, and/or glucose, since these substrates are known to decrease T_2 [20, 27–29]. However, relatively large concentration differences are necessary to bridge the difference between peripheral and ventricular $T_{2,\mathrm{CSF}}$. So although differences in CSF composition may partly cause the observed T_2 difference, it seems unlikely that these are the only contributor.

The shorter in vivo CSF T_2 at 7 T than at 3 T (Fig. 4a) is in line with published in vivo measurements by Daoust et al. [20]. However, Daoust et al. suggested that the T_2 of CSF is not field strength dependent, but that residual field gradients cause errors in in vivo measurements at higher field strengths. If the T_2 measurements are strongly dependent on residual gradients, one might expect that the T_2 difference between periphery and ventricles observed at 3 T is also largely due to residual field gradients, such as $\boldsymbol{B}_0$ gradients. However, the CSF T_2 mapping sequence used in our study showed negligible $\boldsymbol{B}_0$ gradient dependency for the measured T_2 up to 0.3 mT/m, while the observed $\boldsymbol{B}_0$ gradients in the brain were between 0.07 and 0.38 mT/m, and on average well below 0.20 mT/m. The limited diffusion sensitivity of the CSF T_2 mapping sequence is also visible from the results of the long TE analysis on the phantom measurements. The measured T_2 remained unchanged when only long TEs (with stronger diffusion weighting) were used (see Fig. 6).

Implications

Before CSF T_2 mapping can be used as a parameter to study diseases such as cerebral small vessel disease, several uncertainties need to be resolved. It is not yet clear to what extent the T_2 difference between ventricular and peripheral CSF reflects physiological differences in CSF composition. The CSF T_2 mapping sequence shows a much smaller T_2 difference compared with SE-EPI, while the difference also varies with field strength. Overall, the T_2 difference between peripheral and ventricular CSF could (partly) be explained by (a combination of) physiological differences. The possibility that the shorter peripheral T_2 is entirely caused by an artifact, like B_0 gradients caused by imperfect shimming and/or partial volume effects between tissue, blood, and CSF, seems unlikely.

Care should be taken when one is interpreting T_2 measurements of CSF, and more work is necessary to find the true explanations for the T_2 differences between 3 and 7 T and between the peripheral and ventricular CSF at 3 T.

Limitations

The major limitation of this work is that it is an observational study, which limits the extent to which underlying mechanisms causing the observations can be identified. Despite our efforts to separate the effects of partial volume and true physiological differences, it remains uncertain to what extent the observed shorter peripheral $T_{2,\mathrm{CSF}}$ is due to different CSF compositions.

Furthermore, the statistical power of this study was limited by the low number of volunteers combined with the stringent R^2 criterion, which resulted in a relatively large dropout of ROIs.

Moreover, only macroscopic $\boldsymbol{B}_0$ gradients could be determined in the in vivo scans, and the magnitude of microscopic, subvoxel $\boldsymbol{B}_0$ gradients remains unknown.

Finally, no in vitro CSF sample was used to validate the in vivo measurements. In vitro CSF is prone to changes in, for example, O_2 content, compared with in vivo CSF, which may induce T_2 differences between in vitro and in vivo CSF.

Conclusion

CSF T_2 mapping with a dedicated sequence is feasible at both 3 and 7 T, and yields shorter CSF T_2 times at 7 T compared with 3 T. At 3 T, shorter T_2 times were found for peripheral CSF compared with ventricular CSF; at 7 T this effect was much smaller. Partial volume effects can partly explain this T_2 difference, but a physiological contribution to the difference in T_2 between ventricular and peripheral CSF is possible. The different results for different sequences and field strengths, and the confounding influence of partial volume, will make it challenging to accurately isolate and quantify any true physiological effect for applications in research focusing on in vivo evaluation of the (regional) composition of CSF.

Funding The research leading to these results received funding from the European Research Council (ERC) under the European Union's Seventh Framework Programme (2007-2013)/ERC grant agreement no. 337333 (SmallVesselMRI), and the European Union's Horizon 2020 program/ERC grant agreement no. 637024 (HEARTOFSTROKE) and under grant agreement no. 666881 (SVDs@target).

Authors' contribution JMS: Protocol/project development, Data collection, Data analysis. ETP: Protocol/project development, Data analysis. JH: Protocol/project development, Data analysis. PL: Protocol/project development. JJMZ: Protocol/project development, Data collection, Data analysis.

Compliance with ethical standards

Conflict of interest The authors declare that they have no competing interests.

Ethical approval All procedures performed in studies involving human participants were in accordance with the ethical standards of the institutional and/or national research committee and with the 1964 Helsinki declaration and its later amendments or comparable ethical standards.

Informed consent Informed consent was obtained from all individual participants included in the study.

References

1. Qin Q (2011) A simple approach for three-dimensional mapping of baseline cerebrospinal fluid volume fraction. Magn Reson Med 65:385–391
2. Iliff JJ, Wang M, Liao Y, Plogg BA, Peng W, Gundersen GA, Benveniste H, Vates GE, Deane R, Goldman SA, Nagelhus EA, Nedergaard M (2012) A paravascular pathway facilitates CSF flow through the brain parenchyma and the clearance of interstitial solutes, including amyloid β. Sci Transl Med 4:147ra111
3. Iliff JJ, Nedergaard M (2013) Is there a cerebral lymphatic system? Stroke 44:2013–2016
4. Xie L, Kang H, Xu Q, Chen MJ, Liao Y, Thiyagarajan M, O'Donnell J, Christensen DJ, Nicholson C, Iliff JJ, Takano T, Deane R, Nedergaard M (2013) Sleep drives metabolite clearance from the adult brain. Science 342:373–377
5. Spector R, Robert Snodgrass S, Johanson CE (2015) A balanced view of the cerebrospinal fluid composition and functions: focus on adult humans. Exp Neurol 273:57–68
6. De Bresser J, Brundel M, Conijn MM, Van Dillen JJ, Geerlings MI, Viergever MA, Luijten PR, Biessels GJ (2013) Visual cerebral microbleed detection on 7 T MR imaging: reliability and effects of image processing. Am J Neuroradiol 34:E61–E64
7. van Veluw SJ, Biessels GJ, Luijten PR, Zwanenburg JJM (2015) Assessing cortical cerebral microinfarcts on high resolution MR images. J Vis Exp 105:e53125
8. Wisse LEM, Biessels GJ, Heringa SM, Kuijf HJ, Koek DL, Luijten PR, Geerlings MI (2014) Hippocampal subfield volumes at 7 T in early Alzheimer's disease and normal aging. Neurobiol Aging 35:2039–2045
9. Saekho S, Boada FE, Noll DC, Stenger VA (2005) Small tip angle three-dimensional tailored radiofrequency slab-select pulse for reduced B1 inhomogeneity at 3 T. Magn Reson Med 53:479–484
10. De Vis JB, Zwanenburg JJ, van der Kleij LA, Spijkerman JM, Biessels GJ, Hendrikse J, Petersen ET (2015) Cerebrospinal fluid volumetric MRI mapping as a simple measurement for evaluating brain atrophy. Eur Radiol 26:1254–1262
11. Golay X, Petersen ET, Hui F (2005) Pulsed star labeling of arterial regions (PULSAR): a robust regional perfusion technique for high field imaging. Magn Reson Med 53:15–21
12. Levitt MH, Freeman R, Frenkiel T (1982) Broadband heteronuclear decoupling. J Magn Reson 47:328–330
13. Rooney WD, Johnson G, Li X, Cohen ER, Kim SG, Ugurbil K, Springer CS Jr (2007) Magnetic field and tissue dependencies of human brain longitudinal $^{1}H_2O$ relaxation in vivo. Magn Reson Med 57:308–318
14. Pruessmann KP, Weiger M, Scheidegger MB, Boesiger P (1999) SENSE: sensitivity encoding for fast MRI. Magn Reson Med 42:952–962
15. Dale BM, Brown MA, Semelka RC (2015) MRI basic principles and applications, 5th edn. Wiley, Hoboken
16. Yarnykh VL (2007) Actual flip-angle imaging in the pulsed steady state: a method for rapid three-dimensional mapping of the transmitted radiofrequency field. Magn Reson Med 57:192–200
17. MacKay A, Laule C, Vavasour I, Bjarnason T, Kolind S, Mädler B (2006) Insights into brain microstructure from the T_2 distribution. Magn Reson Imaging 24:515–525
18. Cox E, Gowland P (2008) Measuring T_2 and T_2' in the brain at 1.5 T, 3 T and 7 T using a hybrid gradient echo-spin echo sequence and EPI. In: Proceedings of the 16th annual meeting of ISMRM, Toronto, Canada, p 1411
19. Whittall KP, Mackay AL, Graeb DA, Nugent RA, Li DKB, Paty DW (1997) In vivo measurement of T_2 distributions and water contents in normal human brain. Magn Reson Med 37:34–43
20. Daoust A, Dodd S, Nair G, Bouraoud N, Jacobson S, Walbridge S, Reich DS, Koretsky A (2017) Transverse relaxation of cerebrospinal fluid depends on glucose concentration. Magn Reson Imaging 44:72–81
21. Yamada S, Ishikawa M, Yamamot K (2015) Optimal diagnostic indices for idiopathic normal pressure hydrocephalus based on the 3D quantitative volumetric analysis for the cerebral ventricle and subarachnoid space. Am J Neuroradiol 36:2262–2269
22. Stanisz GJ, Odrobina EE, Pun J, Escaravage M, Graham SJ, Bronskill MJ, Henkelman RM (2005) T_1, T_2 relaxation and magnetization transfer in tissue at 3 T. Magn Reson Med 54:507–512
23. Visser F, Zwanenburg JJM, Hoogduin JM, Luijten PR (2010) High-resolution magnetization-prepared 3D-FLAIR imaging at 7.0 tesla. Magn Reson Med 64:194–202
24. Chen JJ, Pike GB (2009) Human whole blood T_2 relaxometry at 3 tesla. Magn Reson Med 61:249–254
25. Krishnamurthy LC, Liu P, Xu F, Uh J, Dimitrov I, Lu H (2014) Dependence of blood T_2 on oxygenation at 7 T: in vitro calibration and in vivo application. Magn Reson Med 71:2035–2042
26. van Veluw SJ, Fracasso A, Visser F, Spliet WGM, Luijten PR, Biessels GJ, Zwanenburg JJM (2015) FLAIR images at 7 tesla MRI highlight the ependyma and the outer layers of the cerebral cortex. Neuroimage 104:100–109

27. Hopkins AL, Yeung HN, Bratton CB (1986) Multiple field strength in vivo T_1 and T_2 for cerebrospinal fluid protons. Magn Reson Med 3:303–311
28. Yilmaz A, Ulak FŞ, Batun MS (2004) Proton T_1 and T_2 relaxivities of serum proteins. Magn Reson Imaging 22:683–688
29. Yadav NN, Xu J, Bar-Shir A, Qin Q, Chan KWY, Grgac K, Li W, McMahon MT, van Zijl PCM (2014) Natural D-glucose as a biodegradable MRI relaxation agent. Magn Reson Med 72:823–828